Results in Physics 37 (2022) 105513

Contents lists available at ScienceDirect

Results in Physics

journal homepage: www.elsevier.com/locate/rinp

Fifth-order nonlinear optical response of Alq_3 thin films

Ahmad Saleh [a], Weiwei Li [b,c], Hadi ALQahtani [d], Marcel Neuhaus [c], Ali Alshehri [e], Boris Bergues [b,c], Meshaal Alharbi [a], Matthias F. Kling [b,c], Abdallah M. Azzeer [a], Zilong Wang [b,c], Abdullah F. Alharbi [f,*]

[a] Attosecond Science Laboratory, Physics and Astronomy Department, King Saud University, Riyadh 11451, Saudi Arabia
[b] Max Planck Institute of Quantum Optics, 85748 Garching, Germany
[c] Physics Department, Ludwig-Maximilians-Universität Munich, 85748 Garching, Germany
[d] Physics and Astronomy Department, King Saud University, Riyadh 11451, Saudi Arabia
[e] Department of Physics, College of Science, King Khalid University, Abha 61413, Saudi Arabia
[f] King Abdulaziz City for Science and Technology (KACST), Riyadh 11442, Saudi Arabia

ARTICLE INFO

Keywords:
Alq_3 films
Tris-(8-hydroxyquinoline) aluminium
Fifth-order nonlinear susceptibility
Fifth-order harmonic generation
Nonlinear absorption

ABSTRACT

The fifth-order optical nonlinearity of Tris-(8-hydroxyquinoline) aluminium (Alq_3) thin films deposited on quartz substrates when exposed to an intense laser excitation of mid-infrared femtosecond pulses is investigated. This property was examined by generating the fifth-harmonic frequency of the driving field whose signal strength as a function of laser intensity is well described by a power-law scaling. The perturbative nature of the underlying mechanism enabled the linking of the process directly to the fifth-order nonlinear optical susceptibility $\chi^{(5)}$. We also utilized the open-aperture z-scan for studying the nonlinear absorption aspect of the third-order nonlinear optical properties of the sample. It was found that Alq_3 thin-films inherit the same saturable absorption character reported in Alq_3 solutions under continuous laser excitation in the visible range, with a comparable value of the nonlinear absorption coefficient β_{eff} (in the order of 10^{-2} cm/W).

Introduction

Organic materials are known to have a great potential for their use as nonlinear optical (NLO) materials in integrated optical and electro-optical devices [1–3]. In addition to ease of fabrication and tailoring ability, these systems are of major interest due to their fast response to light, which is determined by the individual molecular units rather than the bulk electronic structure. Organic materials featuring extended π-electron systems play a central role in this field, where the presence of loosely bound and spatially delocalized electrons results in fast and strong polarization [4,5]. This kind of structure has been employed and proposed in various nonlinear optics-related applications such as optical limiting, saturable absorption, all-optical switches, and harmonic generation [6–11].

The presence of a metal ion in the middle of a highly delocalized π-conjugation system can enrich particular NLO processes. Tris (8-hydroxyquinoline) aluminum (III), abbreviated as (Alq_3), is a well-known example of this type of organometallic structure. Alq_3 is widely involved in various cutting-edge optoelectronic technologies such as organic light-emitting diodes (OLED) and organic light-emitting transistors devices [11–17].

A recent study [18] investigated the optical nonlinearity of Alq_3 in solution form and discussed its potential as a saturable absorber in photonics applications by studying its response to a visible continuous wave (CW) laser using the z-scan technique. The authors reported that the nonlinear absorption coefficient (β_{eff}) has negative values in Alq_3 chloroform solutions under CW excitation in the range from 457 nm to 496 nm. This nonlinear indicator was found to increase with increasing laser power or solution concentration and vary with the tuning of the driving wavelength. In addition to these parameters, the NLO properties are also sensitive to the form of the nonlinear medium. It has been observed [19], for example, that the nonlinear absorption nature of Tetraphenyl-porphyrin (TPP) displays a shift from reverse saturation absorption in TPP solution to saturation absorption in TPP ultrathin films. Thin films of organic materials were also found to provide an excellent platform to modulate the nonlinear response by, for example, defects, grain size, surface morphology, the length of the medium, and the electronic band structure [20–22]. Thin films can offer a compact

* Corresponding author.
E-mail address: harbi@kacst.edu.sa (A.F. Alharbi).

https://doi.org/10.1016/j.rinp.2022.105513
Received 7 February 2022; Received in revised form 30 March 2022; Accepted 11 April 2022
Available online 12 April 2022
2211-3797/© 2022 The Authors. Published by Elsevier B.V. This is an open access article under the CC BY license (http://creativecommons.org/licenses/by/4.0/).

and stable alternative to using solutions in devices where they suffer from practical limitations. Thin films are also considered to be better targets for harmonic generation due to their higher density of emitters. Low-order harmonics such as the third- and fifth- orders are very useful methods for frequency up-conversion, which are important elements for different applications including optical communication and signal processing. Fundamentally, on the other hand, studying low-order harmonics allows for probing materials' key optical constants as well as peculiar electronic properties and dynamics [23–25]. Alq_3 thin films are good candidates for generating low-order harmonics with infrared ultrashort laser pulses due to their high stability, good heat resistance [26], and photophysical properties in the visible region. The unique molecular structure of Alq_3 also facilitates intermolecular charge transfer from ligand to metal and vice versa, in addition to ligand-to-ligand charge transfer, which could enhance NLO polarization. Alq_3 thin-films have been shown to exhibit efficient third-harmonic generation at a fundamental wavelength of 1064 nm in [27,28]. However, beyond third-order nonlinearity, there is a lack of studies on the NLO properties of Alq_3 thin films.

In this work, the nonlinear response of Alq_3 thin films on quartz substrates is studied. Our work first answers the question whether an Alq_3 thin film preserves the saturation absorption character observed in Alq_3 chloroform solutions by measuring its nonlinear absorptive response. Then, a further investigation on the harmonic generation capability of Alq_3 thin-films beyond third-order NLO effects is presented. We report the observation of fifth-order nonlinearity in Alq_3 thin films through the generation of the fifth harmonic frequency in response to a strong laser excitation of 2 μm femtosecond laser pulses. The perturbative character of the process is confirmed and the harmonic yield is linked to the fifth-order NLO susceptibility $\chi^{(5)}$.

Experimental

Film preparation and characterization

Alq_3 powder of purity 99.99% (from Aldrich Chem Co.) with the molecular formula $Al(C_9H_6NO)_3$ was used as received without any further purification.

Alq_3 films were deposited onto pre-cleaned glass and optically flat single-crystal quartz substrates using a conventional thermal evaporation system (Edwards, E 306 A) under a base pressure of 10^{-6} mbar. Glass substrates were used for structural analysis, whereas quartz substrates were used for optical measurements. Both types of substrates were carefully washed several times using acetone, ethyl alcohol, and distilled water separately and then dried with nitrogen gas. The Alq_3 powder was sublimated from a quartz crucible source heated by a tungsten coil at a pressure of 10^{-6} mbar. The deposition rate and film thickness were controlled during the evaporation process using a quartz crystal thickness monitor. The rate of deposition was adjusted to 0.15 nm/s. The thickness of the film was determined after deposition using a DEKTAK thickness profile meter.

The X-ray diffractometer (XRD, X'pert MPD, Panalytical) was used to identify the structural characteristics of the films using Cu K_α radiation of wavelength $\lambda = 1.5406$ A^o as a source. The measurements were performed in the diffraction angle (2θ) range with a step size of 0.02 (2θ/s). The morphology of the films was studied by a field emission scanning electron microscope (JELO JSM-7600F). The UV–visible (UV–Vis) absorption spectra of Alq_3 chloroform solutions and thin films in the wavelength range of 200 to 2000 nm were obtained using a spectrophotometer (JASCO V-670 UV–Vis-NIR). The photoluminescence (PL) emission spectra were carried out using a spectrofluorometer (JASCO FP-8200). Atomic force microscopy (AFM) (Solver Next, NT-MDT, Moscow, Russia) was employed to obtain information on the topography and the surface roughness of the thin film.

Z-scan measurements

The Z-scan technique allows the measurement of the sign and magnitude of third-order NLO quantities, which are critical for practical applications in optical devices. This method, first proposed by Shiek-Bahae et al. [29], records the transmittance of a tightly focused Gaussian beam as a function of the position (z) of the target sample. The nonlinear absorption properties of Alq_3 thin films were measured using the open aperture Z-scan technique with a diode-pumped solid-state (DPSS) laser delivering CW light at 532 nm. In an open aperture (OA) Z-scan, the whole light transmitted through the sample is recorded as a function of its position (z) along the focused laser beam axis.

Fifth-order harmonic generation

The experimental setup employed to generate the fifth-harmonic signal is presented in Fig. 1. The driving mid-infrared laser pulses are produced from an Yb-amplifier pumped optical parametric chirped pulse (OPCPA) [30]. The 100 kHz output beam is linearly polarized with a wavelength centered at around 2 μm and a pulse duration of 30 fs. The laser light is focused into the sample using a concave mirror with a focal length of 20 cm. There was no observed damage in the sample at the maximum laser intensity used in the experiment (2.18 TW/cm^2). The strong signal of the third harmonic in the generated light from the sample overwhelms that of the fifth harmonic. A rotating CaF_2 prism was therefore used to spatially separate the wavelengths. The intensities and spectra of the selected spectral regions from the emitted light were recorded using a photomultiplier tube (PMT) and a UV–VIS spectrometer (Ocean Optics HDX).

Results and discussion

Structural characterization

The X-ray diffraction pattern of the sample is shown in Fig. 2. The broad XRD hump at about $2\theta = 24°$, with no sharp peaks, confirms the amorphous nature of the film.

The surface morphology of the thin film was investigated using a field emission scanning electron microscope (FESEM). The image in Fig. 3(a) indicates that the surface of the thin film is textured with randomly and irregular granules of Alq_3 molecules.

As shown in Fig. 3(b), a two-dimensional surface morphology image of Alq_3 thin film was obtained using an Atomic Force Microscope (AFM).

The surface of the as-deposited thin film was scanned over an area of 5×5 μm^2 and displays arrangement of hills and valleys, with randomly arranged aggregation grains.

Linear optical characterization

The normalized absorption spectrum of Alq_3 thin film is shown in Fig. 4. In the visible region, the film exhibits a weak broad absorption peak centered at around 392 nm. In the ultraviolet (UV) region two

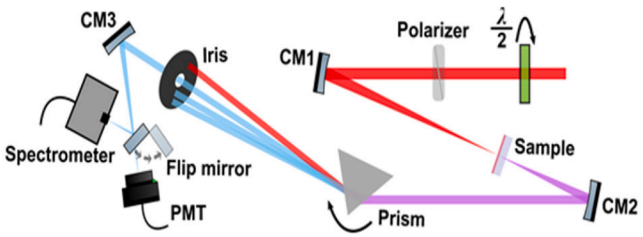

Fig. 1. Schematic diagram of the experimental setup for 5th harmonic generation from Alq_3 thin film in transmission geometry. λ/2: Half wave plate; CM: focusing concave mirror; PMT: photomultiplier tube.

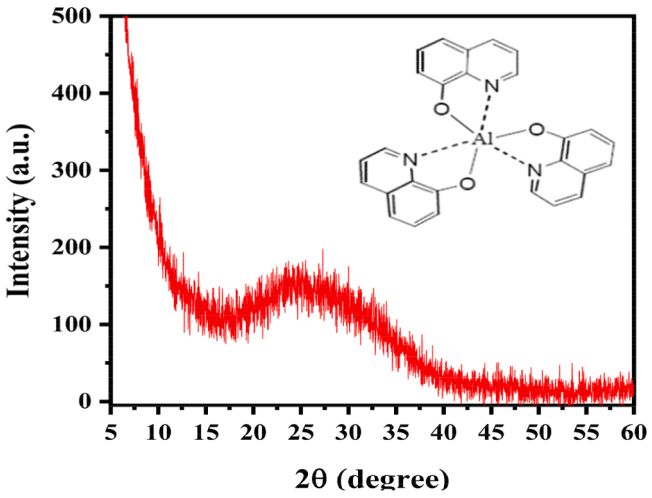

Fig. 2. X-ray diffraction spectrum of Alq_3 thin film. Inset: chemical structure of Alq_3 molecule.

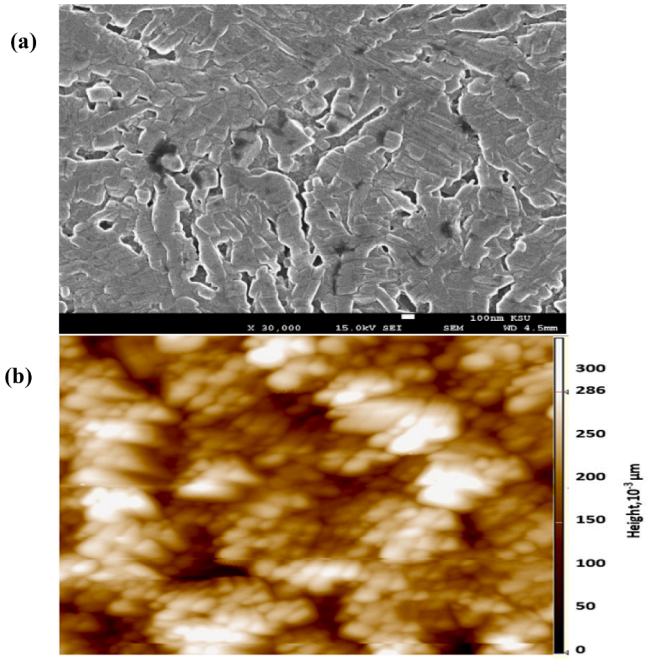

Fig. 3. **(a)** FESEM image of Alq_3 thin film scanned over 100 × 100 nm^2.**(b)** 2D-topograpical Atomic Force Microscopy (AFM) image of Alq_3 thin film from an approximately 5 µm × 5 µm scanned area.

strong narrow absorption peaks can be observed at around 265 nm and 196 nm. The first absorption band in the UV range is known as the Soret (B) band and is due to the ($S_0 \rightarrow S_2$) transition, whereas the absorption band in the visible range is known as the Q band and is due to the ($S_0 \rightarrow S_1$) π-π* transition [31].

The normalized photoluminescence (PL) emission spectrum of the Alq_3 thin film is also shown in Fig. 4. A broad PL spectrum emission peak centered at 509 nm is observed in the spectrum after photo-exciting the sample with an incident wavelength at 390 nm. This broadband emission can be attributed to the ($S_1 \rightarrow S_0$) transition [32].

Nonlinear absorption measurements

The nonlinear absorption coefficient (β_{eff}) is a measure of NLO absorption and is related to the imaginary part of the third-order NLO

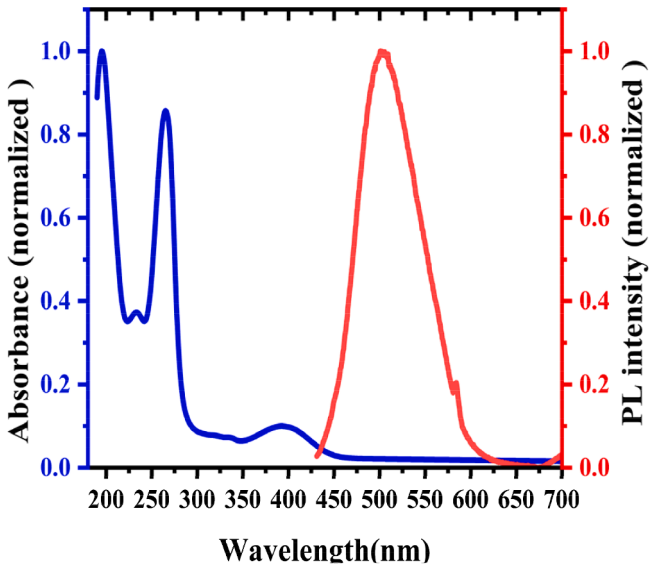

Fig. 4. Normalized UV–Vis absorption (blue curve) and PL spectra (red curve) of 500 nm-thick Alq_3 thin film.

susceptibility $\chi^{(3)}$ (in units of esu) through the following relation [33]:

$$\mathbf{Im}\chi(3) = 10^{-2}\frac{(\varepsilon_0\ \mathbf{c}^2\ \mathbf{n}_0^2\beta_{\mathbf{eff}}\lambda)}{4\pi^2} \quad (1)$$

where ε_0 is the permittivity of free space, c is the velocity of light in vacuum, λ is the wavelength of the laser beam, and n_0 is the linear refractive index.

In general, nonlinear absorption can be attributed to saturation absorption, reverse saturation absorption, or two-photon absorption. The first process is associated with saturation effects and causes a decrease in the absorption of the sample with increasing laser intensity. On the other hand, both reverse saturation absorption and two-photon absorption lead to an increase in absorption due to the involvement of higher excited states with proper lifetimes and cross sections in the process and immediate transition by instantaneous two-photon absorption, respectively [34].

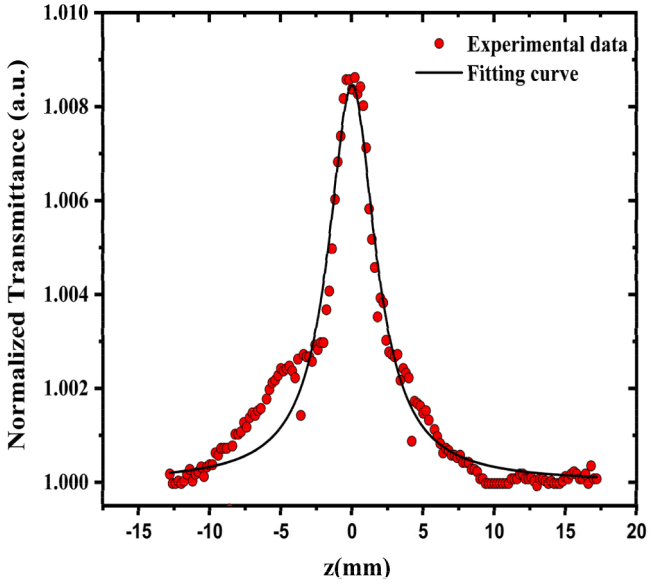

Fig. 5. Experimental data (red circles) and fitted curve (solid black) for the open aperture Z-scan measurement of Alq_3 thin film at the laser wavelength of 532 nm and an intensity of 1.27 × 10^4 w/cm^2.

Fig. 5 shows the normalized experimental OA Z-scan transmittance curve for a 500 nm-thick Alq_3 thin film at a laser wavelength at 532 nm and an intensity of $I_o = 1.27 \times 10^4$ W/cm^2. The measured curve is flat at sample positions away from the focus where linear processes are dominant. Near the focus, the curve exhibits a narrow symmetric bell-shaped profile with a maximum at the focus point (z = 0), which is a signature of saturation absorption. The experimental transmission values of the OA Z-scan can be fitted using the following expression [29,35–39]:

$$\mathbf{T(z)} = \frac{1}{\mathbf{q_0(z)}}\mathbf{ln}(1 + \mathbf{q_0(z)}) \tag{2}$$

where q_0 is a β_{eff} -dependent parameter defined as $q_0(z) = \beta_{eff} I_o L_{eff}/(1 + z^2/z_o^2)$ with L_{eff} and z_0 standing for the effective thickness of the sample and the Rayleigh length of the focused beam, respectively.

The fitted curve is also shown in Fig. 5. The extracted nonlinear absorption coefficient (β_{eff}) is negative, indicating the saturation absorption nature of the sample. The estimated values of β_{eff} and $Im(\chi^{(3)})$ for the Alq_3 thin films are found to be $-2.84 \pm 0.30 \times 10^{-2}$ cm/W and $-9.95 \pm 1.49 \times 10^{-6}$ esu, respectively.

The response of the thin film at 532 nm exhibits the same nonlinear absorptive character observed in Alq_3 chloroform solutions [18]. Moreover, the numerical values of β_{eff} in both forms are within the same range ($\beta_{eff} \approx -2.5 \times 10^{-2}$ cm/W in Alq_3 chloroform solutions).

Fifth-order nonlinear optical measurements

To produce the 5th harmonic signal from a 500 nm thick Alq_3 film, femtosecond laser pulses with a central wavelength of around 2 μm are used. Fig. 6(a) shows the 5th harmonic order spectrum from the Alq_3 thin film plotted in red. The figure also presents the spectrum obtained from the bare quartz substrate in black, which is less intense by an order of magnitude. Therefore, it can be inferred that the dominant contribution to the harmonic signal from the sample originates from the organic layer while the background signal from the substrate has only a little influence.

In the following, we show how the measured harmonic yield can be related quantitatively to the fifth-order susceptibility $\chi^{(5)}$. First, Fig. 6(b) displays the fifth harmonic intensity (blue dots) in the Alq_3 thin film as a function of excitation intensity plotted on a double logarithmic scale.

The experimentally measured harmonic signal (S_{exp}) is fitted by the following relation:

$$S_{exp} = \eta I^5 = \eta\left(\frac{C\varepsilon_0 E^2}{2}\right)^5 \tag{3}$$

where E is the electric field and η is a proportionality constant. The constants c and ε_0 are the speed of light and the vacuum permittivity, respectively.

The above power-law scaling of the fifth harmonic suggests the perturbative nature of the generation process resulting from multi-photon absorption [40]. In this regime, the time-dependent polarization along the laser direction, neglecting tensorial and non-instantaneous effects, can be written as [41]:

$$p(t) = \varepsilon_0 V_{focal} \sum_i \chi^{(i)}.E^i(t) \tag{4}$$

where $\chi^{(N)}$ is the susceptibility of order N, and V_{focal} is the focal volume.

The calculated harmonic signal (S_{calc}) is given by the 5th component of the Fourier transform of the second time-derivative of polarization [41]: $\left|FT\left\{\frac{d^2}{dt^2}p(t)\right\}\right|^2$.

To extract this component, we use the expansion.

$$E^i(t) = E_0^i cos^i(\omega_0 t) = E_0^i \sum_{j=1}^{i} a_j \cos(j\omega_0 t) \tag{5}$$

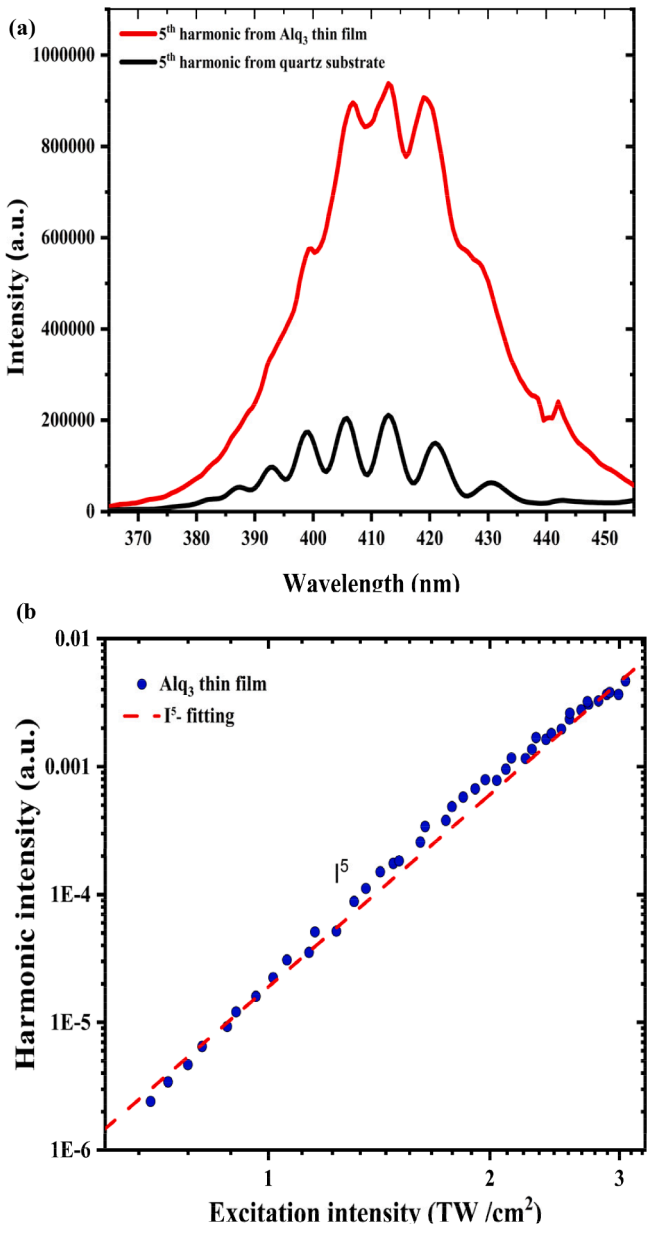

Fig. 6. (a) Fifth harmonic spectra from 500 nm Alq_3 thin films and 500 μm quartz substrate, at an estimated laser intensity of 2.18 TW/cm^2 and a wavelength of 2 μm in the transmission geometry. **(b)** Laser-intensity dependence of the strength of the 5th harmonic signal.

to express the fifth order of polarization in the following form:

$$p_5(t) = \varepsilon_0 V_{focal} \chi^{(5)} E_0^5 \cos(5\omega_0 t) \tag{6}$$

Thus, the expression for S_{calc} can be obtained as:

$$S_{calc} = \gamma |\chi^{(5)}|^2 E_0^{10} = \gamma \left(\frac{2}{c\varepsilon_0}\right)^5 |\chi^{(5)}|^2 I^5 \tag{7}$$

where γ contains all pre-factors. Equating S_{exp} and S_{calc}, one can extract the value of $\chi^{(5)}$:

$$\chi^{(5)} = \sqrt{\left(\frac{c\varepsilon_0}{2}\right)^5 \frac{\eta}{\gamma}} \tag{8}$$

This relation shows that $\chi^{(5)}$ is directly linked to the harmonic yield through the proportionality constant η. One can calculate the exact

value of $\chi^{(5)}$ from Eq. (8) using the value of η only if the units of the harmonic intensity are not arbitrary. However, we can have a rough estimate of the value of $\chi^{(5)}$ using the well-known numerical ratio connecting successive susceptibilities [40]:

$$\frac{\chi^{(N)}}{\chi^{(N+2)}} \; 10^{-20} \tag{9}$$

Assuming that the reported measure value of $\chi^{(3)} = 1.32 \times 10^{-20}\ m^2/V^2$ obtained using the rotational maker finger technique in [28] varies slowly with wavelength, $\chi^{(5)}$ can be estimated to be in the order of $10^{-40}\ m^2/V^2$. Given that the relatively strong linear absorption coefficient of Alq_3 thin film ($\alpha = 1.67 \times 10^6\ m^{-1}$) in the range of the fifth harmonic frequency, we expect the fifth-order nonlinear response of the film to be higher than the estimated value. The observation that Alq_3 has a noticeable fifth-order harmonic signal at 2 μm aligns with the prediction of enhanced induced polarization due to the presence of a central metal atom in the highly delocalized π-conjugation system [28,42].

Conclusion

The nonlinear absorption and fifth-order harmonic generation were studied in tris-(8-hydroxyquinoline) aluminium (Alq_3) thin films.

The X-ray diffraction pattern revealed the amorphous nature of the film structure. The optical properties of Alq_3 thin films were examined using spectrometric measurements at nearly normal incidence of light in the wavelength range of (200–2500) nm. The negative value of the absorption coefficient (β_{eff}) obtained from the Z-scan measurement at 532 nm confirmed the saturation absorption property of the films. Under mid-infrared femtosecond pulses, Alq_3 thin films exhibited a noticeable fifth harmonic response, which was confirmed to be of perturbative nature. The measured NLO properties of Alq_3 thin films present great potential for use in optoelectronic applications.

CRediT authorship contribution statement

Ahmad Saleh: Conceptualization, Data curation, Methodology, Software, Visualization, Writing – original draft. **Weiwei Li:** . **Hadi ALQahtani:** Conceptualization, Writing – review & editing. **Marcel Neuhaus:** . **Ali Alshehri:** Data curation, Writing – review & editing. **Boris Bergues:** . **Meshaal Alharbi:** Writing – review & editing. **Matthias F. Kling:** . **Abdallah M. Azzeer:** Supervision, Investigation, Methodology, Writing – review & editing. **Zilong Wang:** . **Abdullah F. Alharbi:** Supervision, Investigation, Conceptualization, Data curation, Methodology, Validation, Visualization, Data curation, Writing – original draft.

Declaration of Competing Interest

The authors declare that they have no known competing financial interests or personal relationships that could have appeared to influence the work reported in this paper.

Acknowledgments

The authors would like to thank Deanship of scientific research in King Saud University for funding and supporting this research through the initiative of DSR Graduate Students Research Support (GSR).

The authors also thank Amjad Mathhar and Ahmad Alqarni for fruitful discussion and technical assistance.

The MPQ/LMU group acknowledges support within the MPQ-KSU collaboration. W.L. acknowledges support by the CSC program, and the Max Planck Society via the IMPRS for Advanced Photon Science. Z. Wang is grateful for support by a startup grant from the SPP QUTIF funded by the German Research Foundation, and the Alexander von Humboldt foundation.

References

[1] Marder SR. Organic nonlinear optical materials: where we have been and where we are going. Chem Commun 2006;2:131–4.
[2] Munn RW, Ironside C. Principles and applications of nonlinear optical materials. Springer; 1993.
[3] Kasap S. Springer handbook of electronic and photonic materials. Springer Science & Business Media; 2006.
[4] Hunter CA, Sanders JK. The nature of. pi.-. pi. interactions. J Am Chem Soc 1990; 112(14):5525–34.
[5] Ros MB. Organic materials for nonlinear optics. In: Engineering of Crystalline Materials Properties. Springer; 2008. p. 375–90.
[6] Cheng L et al., *Linear and nonlinear optical properties modulation of Sb2Te3/GeTe bilayer film as a promising saturable absorber*. 2019. **13**: p. 102282.
[7] Eevon C et al., *Linear and nonlinear optical properties of Gd3+ doped zinc borotellurite glasses for all-optical switching applications*. 2016. **6**: p. 761-766.
[8] Santos FA, et al. Nonlinear optical study in a set of dibenzylideneacetone derivatives with potential for optical frequency conversion. Photonics. Multidisciplinary Digital Publishing Institute; 2020.
[9] Liu C, et al., *Tunable nonlinear optical absorption in amorphous and crystalline Sb2Se3 thin films*. 2019. **791**: p. 753-760.
[10] Singer K, Lalama S, Sohn J. Organic nonlinear optical materials. Integrated Optical Circuit Engineering II. International Society for Optics and Photonics; 1985.
[11] Calvete M, Yang GY, S.M. Hanack MJ, *Porphyrins and phthalocyanines as materials for optical limiting*. 2004. 141(3): p. 231-243.
[12] Ayobi A, et al., *The effects of MoO3/TPD multiple quantum well structures on the performance of organic light emitting diodes (OLEDs)*. 2019. 30(4): p. 3952-3958.
[13] Ayobi A, et al., *Investigation of charge trapping induced by DCM–TPA dopant in organic light emitting devices composed of (NPB: Alq3): DCM–TPA mixed host-doped emitting layer*. 2019. 20(3): p. 240-251.
[14] Saeed A, Alshahrie A, Salah NJ, *Fabrication of highly efficient organic light-emitting diode based on dysprosium-incorporated tris-(8-hydroxyquinoline) aluminum*. 2020. 31 (24): p. 22179-22189.
[15] Aziz A, Narasimhan K, *Optical absorption in AlQ*. 2000. 114(2): p. 133-137.
[16] Cui C, et al., *Oligonucleotide assisted light-emitting Alq3 microrods: energy transfer effect with fluorescent dyes*. 2013. **49**(47): p. 5360-5362.
[17] Kandulna R, et al., *PMMA–TiO2 based polymeric nanocomposite material for electron transport layer in OLED application*. 2018. **29**(7): p. 5893-5907.
[18] Saeed, A., M.A. Razvi, and N.J.R.i.P. Salah, *Third-order nonlinear optical properties of the small-molecular organic semiconductor tris (8-Hydroxyquinoline) aluminum by CW Z-scan technique*. 2021. **24**: p. 104162.
[19] Clavian L, et al., *Enhanced third order optical nonlinearity in ultrathin amorphous film of tetraphenyl-porphyrin in picosecond regime*. 2019. **119**: p. 105642.
[20] Kajzar F, *Organic thin films for waveguiding nonlinear optics*. Vol. 2. 1996: CRC Press.
[21] Norwood R, Sounik J. Third-order nonlinear optical response in polymer thin films incorporating porphyrin derivatives. Appl Phys Lett 1992;60(3):295–7.
[22] Mattu J, Johansson T, Leach G. Third-order nonlinear optical response from polythiophene-based thin films. J Phys Chem C 2007;111(18):6868–74.
[23] Lafeta L, et al., *Second-and third-order optical susceptibilities in bidimensional semiconductors near excitons states*. 2021.
[24] Konorov S, et al., *Femtosecond optical harmonic generation as a non-linear spectroscopic probe for carbon nanotubes*. 2003. **34**(12): p. 1018-1024.
[25] Ghimire S, Reis DA. High-harmonic generation from solids. Nature Phys 2019;15 (1):10–6.
[26] Yawalkar P, et al., *Photoluminescence of Alq3-and Tb-activated aluminium–tris (8-hydroxyquinoline) complex for blue chip-excited OLEDs*. 2013. **28**(1): p. 63-68.
[27] Zawadzka A, et al., *Photophysical properties of Alq3 thin films*. 2013. **36**(1): p. 91-97.
[28] Popczyk A, et al., *Selected organometallic compounds for third order nonlinear optical application*. 2019. **9**(2): p. 254.
[29] Sheik-Bahae M, et al., *Sensitive measurement of optical nonlinearities using a single beam*. 1990. **26**(4): p. 760-769.
[30] Neuhaus M, et al., *10 W CEP-stable few-cycle source at 2 μm with 100 kHz repetition rate*. 2018. **26**(13): p. 16074-16085.
[31] Muhammad FF, Hapip AIA, Sulaiman KJ. Study of optoelectronic energy bands and molecular energy levels of tris (8-hydroxyquinolinate) gallium and aluminum organometallic materials from their spectroscopic and electrochemical analysis. J Org Chem 2010;695(23):2526–31.
[32] Duvenhage M, Ntwaeaborwa O, Swart HJ. Optical and chemical properties of Alq3: PMMA blended thin films. Mater Today: Proc 2015;2(7):4019–27.
[33] Mathews S, et al. Large third-order optical nonlinearity and optical limiting in symmetric and unsymmetrical phthalocyanines studied using Z-scan. Optics Commun 2007;280(1):206–12.
[34] De Boni L, et al., *Nonlinear optical absorption of organic molecules for applications in optical devices*. 2010: p. 838.
[35] Kwak CH, Lee YL, Kim SG. Analysis of asymmetric Z-scan measurement for large optical nonlinearities in an amorphous As 2 S 3 thin film. J Optical Soc Am B 1999; 16(4):600–4.
[36] Ganeev R, et al., *Nonlinear susceptibilities, absorption coefficients and refractive indices of colloidal metals*. 2001. **34**(11): p. 1602.
[37] Muller O, et al. Optical limiting properties of surface functionalized nanodiamonds probed by the Z-scan method. Sci Rep 2019;9(1):1–11.
[38] Muller O, et al. Synthesis, characterization and nonlinear optical properties of polylactide and PMMA based azophloxine nanocomposites for optical limiting applications. Mater Sci Eng: B 2022;276:115524.
[39] Heidari B, et al., *Reduced Graphene Oxide Thin Film with Strong Optical Nonlinearity*. 2021. **258**(3): p. 2000397.

[40] Boyd RW, *Nonlinear optics*. 2020: Academic press.
[41] Osika EN, et al., *Wannier-Bloch approach to localization in high-harmonics generation in solids.* 2017. **7**(2): p. 021017.
[42] Qian Y, et al., *Synthesis and third-order optical nonlinearities of nickel complexes of 8-hydroxyquinoline derivatives*. 2010. **283**(10): p. 2228-2233.